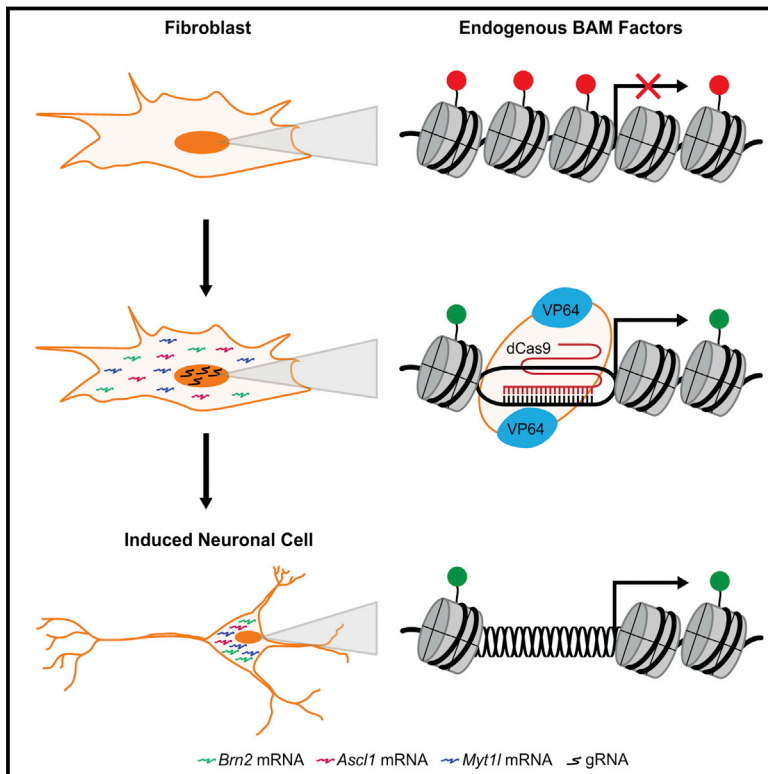


# Cell Stem Cell

## Targeted Epigenetic Remodeling of Endogenous Loci by CRISPR/Cas9-Based Transcriptional Activators Directly Converts Fibroblasts to Neuronal Cells

### Graphical Abstract



### Authors

Joshua B. Black, Andrew F. Adler, Hong-Gang Wang, ..., Geoffrey S. Pitt, Kam W. Leong, Charles A. Gersbach

### Correspondence

charles.gersbach@duke.edu

### In Brief

Black et al. show that reprogramming of fibroblasts to induced neurons via CRISPR/Cas9-based activation of endogenous neurogenic genes leads to rapid epigenetic remodeling at the targeted endogenous loci and sustained gene expression throughout the reprogramming process.

### Highlights

- Multiplexed CRISPR/Cas9 activators induce expression of endogenous neurogenic genes
- Induced endogenous gene expression directly converts fibroblasts to neuronal cells
- Targeted activation of endogenous genes rapidly remodels chromatin at target loci
- High expression from the endogenous genes is sustained throughout reprogramming

# Targeted Epigenetic Remodeling of Endogenous Loci by CRISPR/Cas9-Based Transcriptional Activators Directly Converts Fibroblasts to Neuronal Cells

Joshua B. Black,<sup>1</sup> Andrew F. Adler,<sup>1,9</sup> Hong-Gang Wang,<sup>6,8,10</sup> Anthony M. D'Ippolito,<sup>2,3</sup> Hunter A. Hutchinson,<sup>1</sup> Timothy E. Reddy,<sup>2,4</sup> Geoffrey S. Pitt,<sup>6,7,8</sup> Kam W. Leong,<sup>1,11</sup> and Charles A. Gersbach<sup>1,2,5,\*</sup>

<sup>1</sup>Department of Biomedical Engineering, Duke University, Durham, NC 27708, USA

<sup>2</sup>Center for Genomic and Computational Biology, Duke University, Durham, NC 27708, USA

<sup>3</sup>University Program in Genetics and Genomics, Duke University Medical Center, Durham, NC 27710, USA

<sup>4</sup>Department of Biostatistics and Bioinformatics, Duke University Medical Center, Durham, NC 27710, USA

<sup>5</sup>Department of Orthopaedic Surgery, Duke University Medical Center, Durham, NC 27710, USA

<sup>6</sup>Ion Channel Research Unit, Duke University Medical Center, Durham, NC 27710, USA

<sup>7</sup>Department of Neurobiology, Duke University Medical Center, Durham, NC 27710, USA

<sup>8</sup>Division of Cardiology, Department of Medicine, Duke University Medical Center, Durham, NC 27710, USA

<sup>9</sup>Present address: Department of Neurosciences, University of California, San Diego, La Jolla, CA 92093, USA

<sup>10</sup>Present address: Cardiovascular Research Institute, Weill Cornell Medicine, New York, NY 10021, USA

<sup>11</sup>Present address: Department of Biomedical Engineering, Columbia University, New York, NY 10027, USA

\*Correspondence: [charles.gersbach@duke.edu](mailto:charles.gersbach@duke.edu)

<http://dx.doi.org/10.1016/j.stem.2016.07.001>

## SUMMARY

Overexpression of exogenous fate-specifying transcription factors can directly reprogram differentiated somatic cells to target cell types. Here, we show that similar reprogramming can also be achieved through the direct activation of endogenous genes using engineered CRISPR/Cas9-based transcriptional activators. We use this approach to induce activation of the endogenous *Brn2*, *Ascl1*, and *Myt1l* genes (BAM factors) to convert mouse embryonic fibroblasts to induced neuronal cells. This direct activation of endogenous genes rapidly remodeled the epigenetic state of the target loci and induced sustained endogenous gene expression during reprogramming. Thus, transcriptional activation and epigenetic remodeling of endogenous master transcription factors are sufficient for conversion between cell types. The rapid and sustained activation of endogenous genes in their native chromatin context by this approach may facilitate reprogramming with transient methods that avoid genomic integration and provides a new strategy for overcoming epigenetic barriers to cell fate specification.

## INTRODUCTION

Direct reprogramming of somatic cells has tremendous potential to advance applications in disease modeling, drug discovery, and gene and cell therapies. Common approaches to achieve cellular reprogramming rely on the ectopic expression of transgenes encoding lineage-specific transcription factors (Davis et al., 1987; Takahashi and Yamanaka, 2006; Vierbuchen

et al., 2010). To demonstrate stable cellular reprogramming to an autonomous cell phenotype, the expression of exogenous transcription factors should be transient. Thus the establishment of positive feedback networks regulating endogenous genes is necessary to sustain a transgene-independent cellular identity (Vierbuchen and Wernig, 2011). In many cases, the endogenous genes are occluded by *cis*-acting repressive chromatin marks that are slow to remodel (Vierbuchen and Wernig, 2012). This slow remodeling process typically necessitates prolonged expression of the exogenous factors, limiting the efficacy of transient delivery methods, and poses a major bottleneck to improving the efficiency, speed, and robustness of reprogramming (Hanna et al., 2009).

The type II clustered regularly interspaced short palindromic repeat (CRISPR) system and the CRISPR-associated Cas9 nuclease have recently been repurposed from an adaptive immune system in bacteria and archaea to a gene editing tool (Cong et al., 2013; Jinek et al., 2012; Mali et al., 2013b) and transcriptional regulator (Cheng et al., 2013; Gilbert et al., 2013; Kornemann et al., 2013; Maeder et al., 2013b; Mali et al., 2013a; Perez-Pinera et al., 2013; Qi et al., 2013) of endogenous genes in mammalian cells. The ability to program these transcription factors to target any genomic locus of interest through the simple exchange of the 20-nt targeting sequence of the guide RNA (gRNA) enables a simple, robust, and highly scalable method for control of complex transcriptional networks (Thakore et al., 2016). Furthermore, dCas9-based transcription factors can target stably silenced genes within compacted chromatin to initiate chromatin remodeling and transcriptional activation (Perez-Pinera et al., 2013; Polstein et al., 2015). Thus, this technology may provide a method to deterministically initiate expression of endogenous gene networks of alternate cell lineages.

The CRISPR/Cas9 system and other platforms for programmable transcriptional regulation have been incorporated into methods for cellular reprogramming in a few recent studies. Gao et al. used transcription activator-like effector (TALE)-based

transactivators targeting an enhancer of *Oct4* to generate mouse induced pluripotent stem cells. Notably, that study required co-delivery of vectors directly encoding ectopic *C-MYC*, *KLF4*, and *SOX2* to achieve pluripotency (Gao et al., 2013). More recently, we have demonstrated the direct conversion of primary mouse embryonic fibroblasts (PMEFs) to skeletal myocytes using a dCas9-based transactivator targeting the endogenous *MyoD1* gene (Chakraborty et al., 2014). Several groups have also applied CRISPR/Cas9-based transcriptional regulation to direct the differentiation of human induced pluripotent and embryonic stem cells (Balboa et al., 2015; Chavez et al., 2015; Wei et al., 2016).

The above examples involve the targeted activation of a single transcription factor to guide reprogramming or differentiation, but many approaches require concurrent expression of multiple factors to efficiently establish a mature phenotype (Takahashi and Yamanaka, 2006; Vierbuchen et al., 2010). There have been no examples demonstrating multiplex endogenous gene activation to induce cellular reprogramming, and the versatility of that approach for direct conversion to other cell phenotypes is not known. Moreover, only the report of TALE transcription factors targeting *Oct4* evaluated changes to epigenetic marks at the target loci (Gao et al., 2013), and this group later reported that dCas9-based transcriptional activators were inefficient at endogenous gene activation and reprogramming (Gao et al., 2014). In this study, we tested the hypothesis that targeted epigenetic reprogramming of the regulatory elements controlling expression of lineage-specific transcription factors is sufficient for direct conversion between cell types by applying dCas9-based transactivators to the activation of endogenous genes that directly convert PMEFs to induced neuronal cells (iNs).

## RESULTS

### Multiplex Endogenous Gene Activation of Neurogenic Factors in PMEFs

Overexpression of transgenes encoding the transcription factors *Brn2*, *Ascl1*, and *Myt1l* (BAM factors) has been shown to directly convert cultured PMEFs to functional induced neuronal cells (Vierbuchen et al., 2010). We hypothesized that the targeted activation of the endogenous genes encoding these same factors in their native chromatin context via a dCas9-based transactivator could more rapidly and deterministically remodel the chromatin at the target loci and provide an alternate method to achieve the reprogramming of PMEFs to iNs (Figure 1A). To achieve targeted gene activation, we used a transactivator with both N-terminal and C-terminal VP64 transactivation domains (<sup>VP64</sup>dCas9<sup>VP64</sup>) (Chakraborty et al., 2014) that generated a ~10-fold improvement in activation of *ASCL1* in HEK293T cells at 3 days post-transfection compared to the first-generation dCas9 transcription factor with a single C-terminal VP64 domain (Maeder et al., 2013b; Perez-Pinera et al., 2013) (Figure 1B). We used <sup>VP64</sup>dCas9<sup>VP64</sup> for the remainder of this study.

We used lentiviral delivery to constitutively express <sup>VP64</sup>dCas9<sup>VP64</sup> in PMEFs. Initially, we delivered the gRNAs through transient transfection of plasmid DNA in order to assess stable reprogramming of cell phenotype following transient activity of transactivators. The induction of *Brn2* and *Ascl1* gene expression by <sup>VP64</sup>dCas9<sup>VP64</sup> was attained by delivering

four gRNAs targeted to the putative promoter region directly upstream of the transcription start site (TSS). The decision to deliver four gRNAs for each gene was based on the reported synergistic effects of multiple gRNAs on gene activation (Maeder et al., 2013b; Mali et al., 2013a; Perez-Pinera et al., 2013). The optimal gRNAs were selected from a pool of eight gRNAs through elimination screening (Figure S1A). The gRNAs targeting regions proximal to the TSS of the *Myt1l* locus did not induce detectable levels of activation, but targeting an intronic region directly upstream of the first coding exon of *Myt1l* was sufficient to activate expression (Figure S1B).

Co-transfection of 12 gRNA expression plasmids (CR-BAM), targeting each of the three endogenous BAM factors with 4 gRNAs, into PMEFs stably expressing <sup>VP64</sup>dCas9<sup>VP64</sup> was sufficient to induce transcriptional upregulation of all three endogenous genes when compared to the transfection of a plasmid encoding firefly luciferase (pLuc; Figure 1C). We also detected *Brn2* and *Ascl1* protein expression by western blot (Figure S1C), although we could not detect *Myt1l* protein using commercially available antibodies. In addition to gRNA transfections, we transfected three plasmids encoding the BAM factor transgenes under the control of the EF1 $\alpha$ /HTLV promoter (pBAM) into the same cells and observed a modest increase in the mRNA levels of the corresponding endogenous genes (Figure 1C).

To attain successful reprogramming, it is generally considered necessary to express the exogenous factors at high levels (Vierbuchen and Wernig, 2011). Therefore, we compared the total mRNA and protein levels of *Brn2*, *Ascl1*, and *Myt1l* produced 3 days after CR-BAM and pBAM plasmid transfections (Figures 1D–1F). Despite the higher levels of transcriptional activation from the endogenous loci by CR-BAM (Figure 1C), pBAM transfection generated significantly more total mRNA encoding each BAM factor than induction by CR-BAM, as determined by qRT-PCR (Figure 1D). Quantitation of single-cell protein levels from immunofluorescence staining also revealed significantly higher single-cell levels of *Brn2* and *Ascl1* in cells transfected with pBAM compared to those transfected with CR-BAM (Figures 1E and 1F).

### Induction of Neuronal Cells from PMEFs via <sup>VP64</sup>dCas9<sup>VP64</sup>-Mediated Gene Activation

Treated PMEFs were assayed for neuronal phenotypes as detailed schematically in Figure 2A. We observed an increase in mRNA of the early pan-neuronal marker  $\beta$ III tubulin (*Tuj1*) 3 days after transfection with either pBAM or CR-BAM when compared to a pLuc control (Figure 2B). We cultured the cells for 2 weeks in neurogenic medium and analyzed expression of pan-neuronal markers by immunofluorescence staining. We identified cells with neuronal morphologies that expressed *Tuj1* in populations transfected with CR-BAM (Figure 2C). A subset of *Tuj1*<sup>+</sup> cells also expressed the more mature pan-neuronal marker *Map2* (Figure 2C). The generation of *Tuj1*<sup>+</sup> *Map2*<sup>+</sup> cells with neuronal morphologies following treatment with <sup>VP64</sup>dCas9<sup>VP64</sup> and gRNAs was contingent on the addition of a small-molecule cocktail to the medium that has been used previously for neural differentiation of embryonic stem cells and has been shown to improve the efficiency of the direct conversion of human fibroblasts to neurons when used in parallel

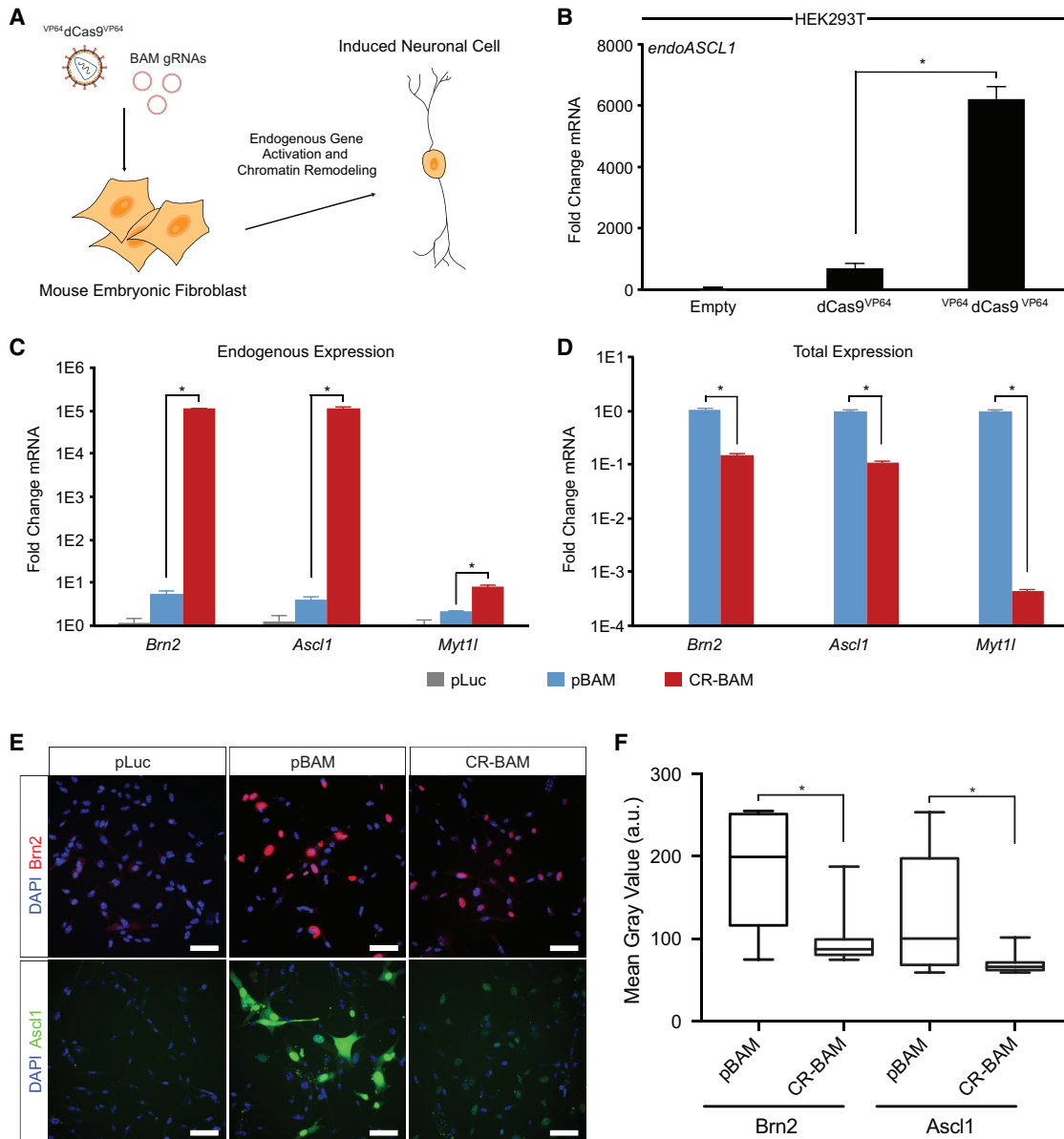


**Figure 1. Endogenous Gene Activation of Neuronal Transcription Factors in PMEFs**

(A) Reprogramming of PMEFs to neuronal cells via transduction of  $VP64$ -dCas9 $^{VP64}$  and transfection of gRNA expression plasmids targeting the endogenous BAM factors.

(B) Transcriptional activation of *ASCL1* in HEK293T cells with dCas9 $^{VP64}$  or  $VP64$ -dCas9 $^{VP64}$  (\*p < 0.05).

(C and D) Endogenous expression (C) and total expression (D) of the BAM factors in PMEFs with targeted activation (CR-BAM) or ectopic overexpression (pBAM; \*p < 0.05).

(E) Immunofluorescence staining of *Brn2* and *Ascl1* in PMEFs demonstrated protein expression through targeted activation of the endogenous loci or expression from ectopic plasmids (scale bar, 50  $\mu$ m).

(F) Automated image analysis of fluorescence intensity revealed significantly more single-cell *Brn2* and *Ascl1* protein with pBAM transfection compared to CR-BAM (\*p < 0.05 between distributions of single-cell mean fluorescence; Z-test).

All gRNAs used are listed in Table S1. All assays were performed on day 3 post-transfection. qRT-PCR data are presented as mean  $\pm$  SEM for n = 3 biological replicates. p values for qRT-PCR data were determined by global one-way ANOVA with Holm-Bonferroni post hoc tests ( $\alpha$  = 0.05). See also Figure S1.

with ectopic expression of neural transcription factors (Ladewig et al., 2012).

We used a lentiviral fluorescent reporter encoding dsRed-Express under the control of the synapsin I promoter (Syn-RFP) as a proxy to define the most functionally mature iNs in

the heterogeneous population of reprogrammed cells (Adler et al., 2012). We readily identified RFP $^{+}$  cells with elaborate arborizations in CR-BAM-transfected PMEFs (Figure 2C). We also identified rare cells with fibroblastic morphologies reactive to the Tuj1 antibody in PMEFs following pLuc transfection

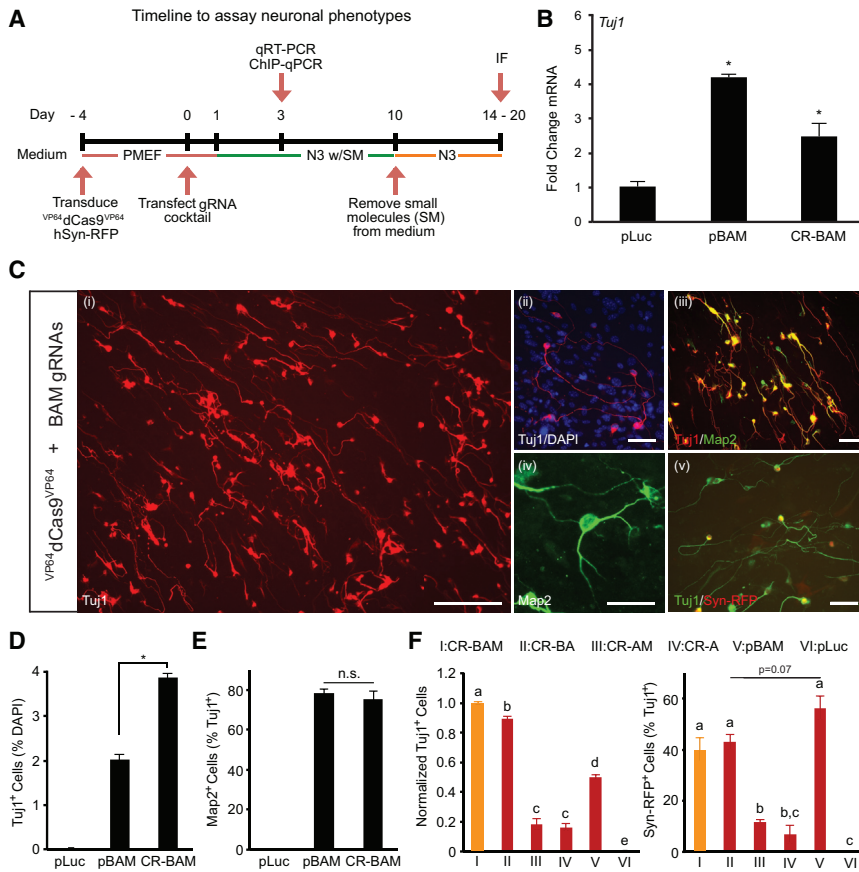


**Figure 2. Induction of Neuronal Cells from PMEFs via  $VP64$ -dCas9- $VP64$ -Mediated Gene Activation**

(A) PMEFs were transduced with a lentivirus encoding the  $VP64$ -dCas9/ $VP64$  transactivator and subsequently transfected with gRNAs targeting *Brn2*, *Ascl1*, and *Myt1l*. Neuronal phenotypes were assayed as indicated.

(B) Transcriptional activation of *TuJ1* was detected in PMEFs at day 3 post-transfection of pBAM or CR-BAM (\* $p < 0.05$  relative to transfection of a plasmid encoding firefly luciferase [pLuc]).

(C) Immunofluorescence staining revealed numerous *TuJ1*<sup>+</sup> cells with neuronal morphologies co-expressing *Map2* at day 14 post-transfection of CR-BAM. The cells with the most elaborate neuronal morphologies activated the synapsin promoter in a Syn-RFP lentiviral reporter (scale bars, 100  $\mu$ m [i], 50  $\mu$ m [ii–v]).

(D) Quantitation of *TuJ1*<sup>+</sup> cells as percent nuclei at day 14 post-transfection of pLuc, pBAM, or CR-BAM (\* $p < 0.05$ ).

(E) Quantitation of *Map2*<sup>+</sup> cells as percent *TuJ1*<sup>+</sup> cells at day 14 post-transfection of pLuc, pBAM, or CR-BAM (n.s., not significant).

(F) Quantitation of *TuJ1*<sup>+</sup> and RFP<sup>+</sup> cells with transfection of different combinations of gRNAs. *TuJ1*<sup>+</sup> cells are normalized to CR-BAM transfection. Conditions that share the same letter (a–e) are not significantly different.

p values were determined by global one-way ANOVA with Holm-Bonferroni post hoc tests ( $\alpha = 0.05$ ). See also Figure S2.

(Figure S2A), but these cells were never reactive to the *Map2* antibody. Consistent with previous studies, direct overexpression of the ectopic BAM factors via transfection of constitutive expression plasmids generated *TuJ1*<sup>+</sup>*Map2*<sup>+</sup> cells with neuronal morphologies (Figure S2B) (Adler et al., 2012; Vierbuchen et al., 2010).

Image analysis revealed that CR-BAM transfection generated a modest, but statistically significant and reproducible, increase in the number of *TuJ1*<sup>+</sup> cells compared to pBAM transfection after 14 days in culture post-transfection (Figure 2D), despite much lower overall expression of the BAM factors (Figures 1D–1F). There was no difference in the percentage of *TuJ1*<sup>+</sup> cells that also expressed *Map2* (Figure 2E). To evaluate the contribution of each neurogenic factor to the generation of *TuJ1*<sup>+</sup> cells and to the level of neuronal maturation, we transfected gRNAs targeting different combinations of the endogenous factors. Removal of gRNAs targeting the *Brn2* locus attenuated iN production ~5-fold when compared to that generated with targeted activation of all three endogenous factors (Figure 2F). We detected a slight reduction in *TuJ1*<sup>+</sup> cell production with the removal of *Myt1l* gRNAs (Figure 2F). Neuronal maturity was assessed as the percentage of *TuJ1*<sup>+</sup> cells co-positive for the Syn-RFP reporter. Removal of *Brn2* gRNAs reduced the percentage of RFP<sup>+</sup> cells >2-fold, but no change was detected with removal of *Myt1l* gRNAs (Figure 2F). pBAM transfection generated a higher percentage of RFP<sup>+</sup> cells than CR-BAM transfection, though it was not statistically significant (Figure 2F).

### Induction of Endogenous Gene Expression Is Rapid and Sustained

For any reprogramming strategy, activation of the endogenous genes encoding the master fate-specifying transcription factors is an important step to the successful reprogramming and stability of the new cellular phenotype (Vierbuchen and Wernig, 2011). Consequently, we compared the kinetics of endogenous gene expression through late stages of reprogramming with pBAM or CR-BAM transfection. We observed activation of all three endogenous genes as early as 1 day post-transfection with CR-BAM that remained at high levels through day 18 in culture (Figure S3A). Expression of the BAM factors from the endogenous loci was significantly higher with targeted activation via CR-BAM compared to ectopic overexpression via pBAM transfection throughout the time course of the experiment. Activation of the endogenous genes by pBAM transfection was delayed, and a significant and sustained increase over baseline levels was only detected for endogenous *Ascl1* and *Myt1l* (Figure S3A).

We next assessed the kinetics of expression of the downstream pan-neuronal marker *TuJ1*. Both pBAM and CR-BAM treatment generated a significant increase in *TuJ1* expression throughout the time course of the experiment (Figure S3B). At early time points, *TuJ1* levels were higher with pBAM treatment than CR-BAM. However, *TuJ1* levels with pBAM treatment peaked 7 days post-transfection and declined thereafter, whereas expression following CR-BAM treatment remained

stable through day 18 in culture (Figure S3B). Importantly, the exogenous BAM factors and gRNAs were significantly depleted by day 18 in culture after transient transfection (Figure S3C), though levels of activation from the endogenous genes remained high in cells treated with CR-BAM (Figure S3A).

### Direct Activation via <sup>VP64</sup>dCas9<sup>VP64</sup> Rapidly Remodels Chromatin at Target Loci

The kinetics of gene activation led us to speculate whether the rapid and sustained elevated levels of endogenous gene expression achieved with CR-BAM corresponded to an altered epigenetic program at the target loci. We used chromatin immunoprecipitation followed by next-generation sequencing (ChIP-seq) data generated as part of the Encyclopedia of DNA Elements (ENCODE) Project (Mouse ENCODE Consortium, 2012) to identify histone modifications enriched at the transcriptionally active BAM factor loci in mouse embryonic brain tissue, including H3K27ac and H3K4me3 (Figures 3A, 3C, and S4A). We hypothesized that targeting the endogenous BAM factors for activation with <sup>VP64</sup>dCas9<sup>VP64</sup> in PMEFs could recapitulate the chromatin signatures found at these loci in developing brain tissue.

To investigate the effects of BAM-factor induction on the epigenetic programming at the target loci, we performed chromatin immunoprecipitation (ChIP) qPCR in PMEFs transduced with <sup>VP64</sup>dCas9<sup>VP64</sup> and transfected with pLuc, pBAM, or CR-BAM plasmids (Figures 3 and S4). We used qPCR primers tiled along intragenic and regulatory regions of the *Brn2*, *Ascl1*, and *Myt1l* loci. We detected a significant enrichment in H3K27ac and H3K4me3 at the *Brn2* and *Ascl1* loci on day 3 post-transfection of CR-BAM (Figures 3B and 3D). H3K4me3 was enriched along the gene bodies of *Brn2* and *Ascl1*. H3K27ac was enriched along the gene bodies and regions surrounding the putative promoter sequences of both genes. In contrast, targeted activation of *Myt1l* only induced modest detectable enrichment in H3K27ac at the gRNA target sites directly upstream of the first coding exon (Figure S4B). No significant change in H3K27ac or H3K4me3 was measured within the putative *Myt1l* promoter. Though overexpression of the BAM factors induced modest levels of expression of the endogenous genes by day 3 post-transfection (Figures 1C and S3A), we did not detect corresponding enrichment in H3K27ac and H3K4me3 at the endogenous loci (Figures 3B, 3D, and S4B).

### Generation of Induced Neuronal Cells with Multiplex gRNA Lentiviral Vectors

To explore a strategy for stable expression of the CRISPR/Cas9 transcription factors, and to see if the same outcomes observed with transient expression held true with constitutive expression, we used a single lentiviral vector capable of expressing four gRNAs from four independent RNA polymerase III promoters (Kabadi et al., 2014) (Figure 4A). Co-transduction of lentiviruses encoding <sup>VP64</sup>dCas9<sup>VP64</sup> and a set of four gRNAs targeting each of the three BAM factors (lentiCR-BAM) permitted concurrent activation of the endogenous BAM factors in PMEFs by day 6 post-transduction (Figure 4B). For comparison, we used lentiviral vectors directly encoding the BAM factors (lentiBAM), and demonstrated activation of the corresponding endogenous genes by day 6 post-transduction (Figure 4B). Similar to the results we obtained

with transient transfection of expression plasmids, targeted activation of the endogenous genes via lentiviral delivery generated significantly more endogenous transcript from the *Brn2* and *Ascl1* loci than that induced through ectopic expression of the BAM factors. However, unlike the transfection experiments, endogenous *Myt1l* expression was significantly higher with transduction of lentiBAM compared to lentiCR-BAM (Figure 4B).

Following extended culture for 2 weeks in neurogenic medium, we readily identified Tuj1<sup>+</sup>Map2<sup>+</sup> cells with complex neuronal morphologies (Figure 4C). All Tuj1<sup>+</sup> cells identified also co-expressed Map2. To promote further neuronal maturation and for electrophysiological assessments, PMEFs were replated onto a previously established monolayer of primary rat astrocytes following transduction of <sup>VP64</sup>dCas9<sup>VP64</sup> and gRNAs (Vierbuchen et al., 2010). Synapsin-RFP expression and cell morphology were used to select the most mature neuronal cells for patch-clamp analysis after 21 days in culture. In current-clamp mode, single or multiple action potentials were readily elicited in response to depolarizing current injections (six out of seven cells analyzed; Figure 4D). The same cells displayed voltage-dependent inward and outward currents. The transient inward currents were abolished in the presence of the voltage-gated Na<sup>+</sup> channel blocker tetrodotoxin (TTX; Figure 4E). The average resting membrane potential, action potential (AP) threshold and AP amplitude were  $-41 \pm 3.8$  mV,  $-33 \pm 2.6$  mV, and  $49 \pm 9.7$  mV, respectively (mean  $\pm$  SEMs, n = 7 cells).

In contrast to what we observed by transient transfection of the reprogramming factors, constitutive expression of the BAM factor transgenes via lentiviral vectors generated significantly more Tuj1<sup>+</sup>Map2<sup>+</sup> cells than that detected with <sup>VP64</sup>dCas9<sup>VP64</sup> (Figure 4F). We hypothesized that the prolonged and high levels of expression of the BAM factor transgenes enabled by lentiviral delivery permitted further epigenetic and transcriptional reprogramming that improved the efficiency of iN generation when compared to transient transfection methods. Consequently, we revisited the analysis of chromatin remodeling at the endogenous BAM factor loci in the context of lentiviral delivery of the reprogramming factors. We found that, as shown with transient transfection, targeted activation of the endogenous genes via lentiCR-BAM transduction led to the rapid deposition of H3K27ac at the *Brn2* and *Ascl1* loci as early as day 3 post-transduction that persisted at day 6 (Figure 4G). Also, as seen with transient transfection, we did not detect enrichment of H3K27ac at the *Myt1l* locus with lentiCR-BAM transduction, although we did measure an increase in *Myt1l* mRNA (Figures 4B and 4G). In contrast to what we observed with transient transfection of the BAM factors, we detected enrichment of H3K27ac along regions of all three endogenous genes with lentiBAM transduction (Figure 4G). Furthermore, we only detected minor enrichment in H3K27ac at all three genes at day 3 post-transduction of lentiBAM; however, both *Ascl1* and *Myt1l* showed a substantial increase in H3K27ac deposition by day 6 post-transduction (Figure 4G).

## DISCUSSION

In this study, we demonstrate direct cellular reprogramming to induced neuronal cells through targeted activation of endogenous genes. We utilized the CRISPR/Cas9 system as a programmable, locus-specific transcriptional regulator for the

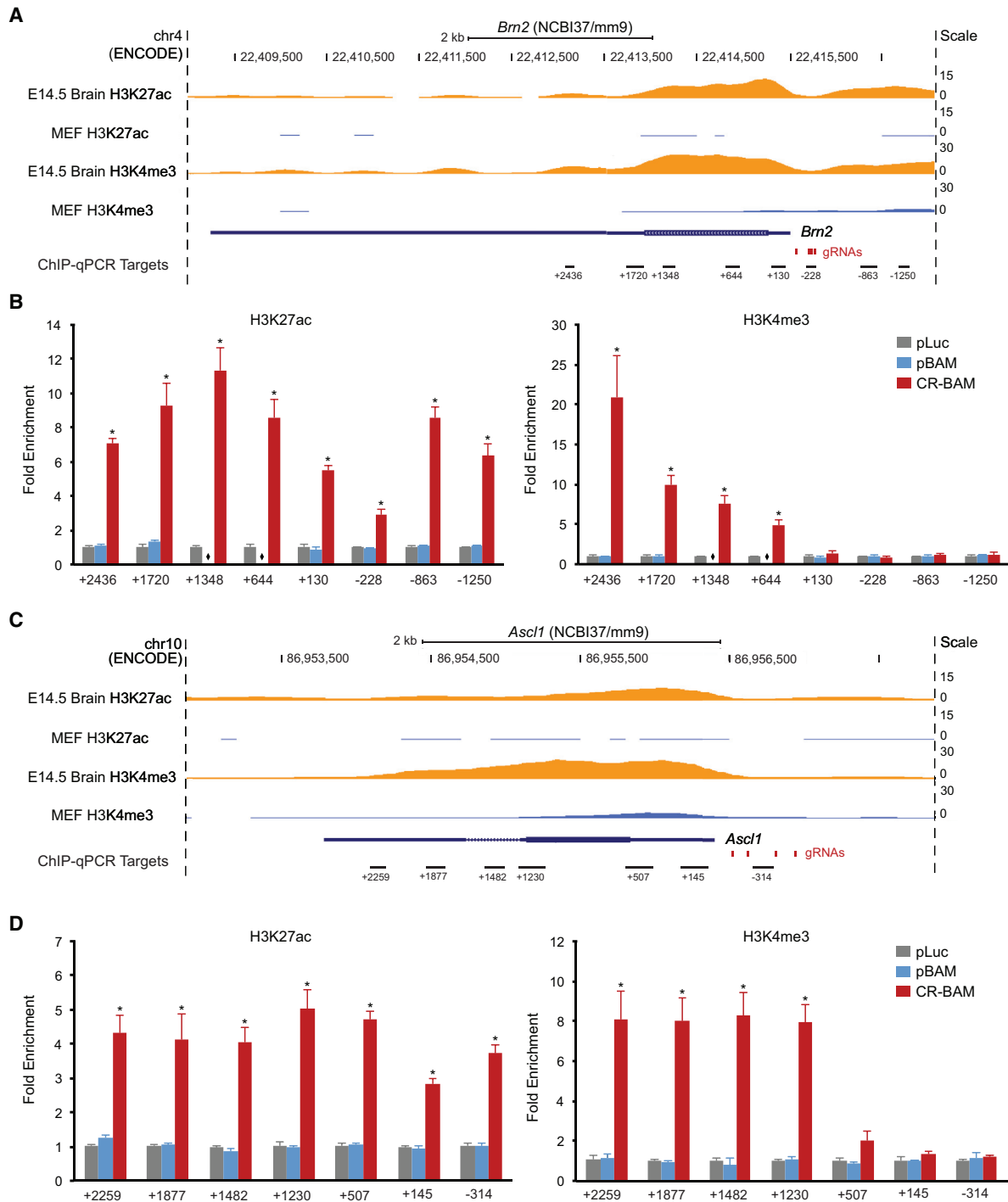


### Figure 3. *VP64*dCas9<sup>VP64</sup> Rapidly Remodels Epigenetic Marks at Target Loci

(A and C) Mouse genomic tracks depicting histone H3 modifications H3K27ac and H3K4me3 at the *Brm2* and *Ascl1* loci in embryonic brain tissue and fibroblasts (data from Mouse ENCODE; GEO: GSE31039). Red bars indicate gRNA target sites near the transcription start site, and black bars indicate the location of ChIP-qPCR amplicons along the gene locus.

(B and D) Targeted activation of endogenous *Brm2* and *Ascl1* in PMEFs induced significant enrichment of H3K27ac and H3K4me3 at multiple sites along the genomic loci at day 3 post-transfection ( $p < 0.05$ , one-way ANOVA with Holm-Bonferroni post hoc tests,  $n = 3$  biological replicates). Overexpression of the BAM factors via transfection of expression plasmids encoding BAM factor transgenes did not induce a significant change in these chromatin marks. qPCR primers targeting coding regions of the genes are not included for the pBAM transfection condition, as contaminating plasmid DNA biased enrichment values, and are marked with diamonds in (B). All fold enrichments are relative to transfection of a plasmid encoding firefly luciferase and normalized to a region of the *Gapdh* locus. See also Figure S3 and S4.

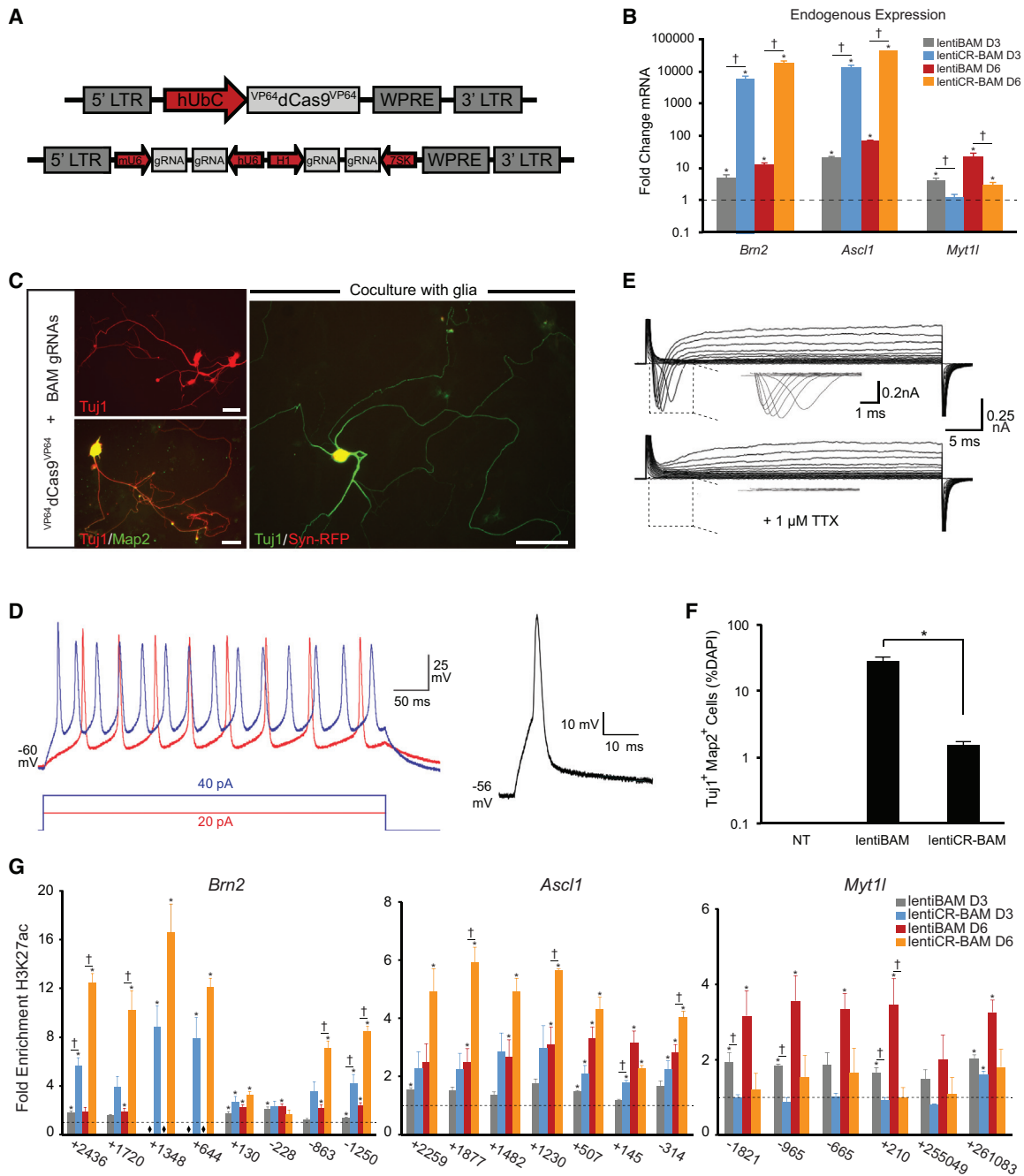


**Figure 4. Generation of Functionally Mature iNs with Multiplex gRNA Vectors**

(A) Schematic of  $VP64dCas9^{VP64}$  and multiplex gRNA lentiviral constructs used to enable stable integration and constitutive expression.

(B) Relative mRNA expression of the endogenous BAM factors following transduction of transgenes encoding the BAM factors (lentiBAM) or  $VP64dCas9^{VP64}$  and gRNAs targeting the endogenous BAM factors (lentiCR-BAM;  $*p < 0.05$  relative to non-treated PMEFS;  $\ddagger p < 0.05$  between lentiBAM versus lentiCR-BAM transduction).

(C) Immunofluorescence staining of PMEFS following transduction of lentiCR-BAM. Cells were co-positive for Tuj1 and Map2 and exhibited complex neuronal morphologies (scale bar, 50  $\mu$ m).

(D) Action potentials were evoked from  $VP64dCas9^{VP64}$ -induced neuronal cells in response to 5-ms (right) or 500-ms (left) step depolarizing current injection (six out of seven cells analyzed) after empiric hyperpolarizing current injection to hold membrane potential at  $\sim -60$  mV.

(E) Representative whole-cell currents recorded with or without perfusion of 1  $\mu$ M tetrodotoxin (TTX).

(F) Quantitation of Tuj1 $^{+}$ Map2 $^{+}$  cells as percent nuclei ( $*p < 0.05$  between lentiBAM versus lentiCR-BAM transduction; NT, non-treated PMEFS).

(G) Time course of H3K27ac enrichment along the *Brn2*, *Ascl1*, and *Myt11* loci ( $*p < 0.05$  relative to non-treated PMEFS;  $\ddagger p < 0.05$  between lentiBAM versus lentiCR-BAM transduction).

All p values calculated by global ANOVA with Holm-Bonferroni post hoc tests ( $\alpha = 0.05$ ).

multiplex activation of the neurogenic factors *Brn2*, *Ascl1*, and *Myt1l* (BAM factors). We hypothesized that targeted activation of the endogenous genes in PMEFS, as opposed to the forced overexpression of the corresponding transgenes, could more directly access the endogenous loci and rapidly remodel their epigenetic signatures, thus potentially reflecting a more natural mechanism of action and serving as an alternate method to achieve cell lineage conversion.

In PMEFS, the *cis*-repressive chromatin landscape at neuronal loci may preclude binding of regulatory factors, in turn impeding transcriptional activation. As a result, expression of the BAM factors in PMEFS from exogenous vectors likely relies on stochastic processes for reactivation of the corresponding endogenous genes. Furthermore, transient delivery of the BAM factors, as done in our initial experiments (Figures 1, 2, and 3), limits the time window within which the endogenous networks and positive feedback loops can be established. We demonstrated that targeting the endogenous genes directly induced the enrichment of histone H3 modifications H3K27ac and H3K4me3 at the *Brn2* and *Ascl1* loci at 3 days post-transfection, whereas transgene overexpression via transfection of plasmids encoding the reprogramming factors did not alter these chromatin marks (Figures 3 and S4). Additionally, we observed sustained high levels of expression from the endogenous genes at later stages of reprogramming despite the transient delivery of the gRNA plasmids (Figure S3).

In contrast, we found that stable integration and constitutive expression of the exogenous reprogramming factors via lentiviral delivery led to the eventual deposition of H3K27ac at their endogenous loci with a concomitant improvement in reprogramming capacity (Figures 4F and 4G). We did not observe a similar improvement with constitutive expression of  $VP64$ -dCas9 $^{VP64}$  and gRNAs, which is possibly attributable to the lower levels of overall expression of the neuronal transcription factors achieved by transactivation of the endogenous genes compared to ectopic overexpression. Consequently, the direct activation of the endogenous genes via  $VP64$ -dCas9 $^{VP64}$  may be more amenable to transient delivery approaches that avoid undesired consequences of vector integration into the genome. Such transient methods, including the direct delivery of ribonucleoprotein Cas9-gRNA complexes, may be a more clinically translatable method of generating reprogrammed cells that are genetically unmodified.

Achieving robust and well-defined reprogrammed cell populations is still a central challenge. Reprogrammed cells often fail to acquire completely mature phenotypes and can retain epigenetic remnants of the native cell type (Kim et al., 2010). Moreover, a recent study demonstrated that reprogramming efficiency can be limited by divergence to a competing cell identity (Treutlein et al., 2016). The molecular mechanisms and practical consequences of these limitations are largely unknown. As the toolkit of designer transcription factors expands to precisely modify the epigenome (Hilton et al., 2015; Kearns et al., 2015; Maeder et al., 2013a; Mendenhall et al., 2013; Thakore et al., 2016), these tools may be used to prime specific genomic loci in diverse cell types, promote endogenous transcription factor binding, and directly correct regions of epigenetic remnants that prove to be problematic for a given application. This may lead to improved reprogramming fidelity and extension of the breadth of donor cells amenable to reprogramming.

## EXPERIMENTAL PROCEDURES

### Cell Culture, Transfections, and Viral Transductions

PMEFS were maintained in high serum media during transduction and transfection of expression plasmids and subsequently cultured in neurogenic serum-free medium for the duration of the experiments to promote neuronal survival and maturation. Lentivirus was produced in HEK293T cells using the calcium phosphate precipitation method. All transfections were performed using Lipofectamine 3000 (Invitrogen) in accordance with the manufacturer's protocol. All expression plasmids used in this study can be found in Table S2.

### Immunofluorescence Staining and qRT-PCR

All sequences for qRT-PCR primers can be found in Table S3. Total RNA was isolated using the QIAGEN RNeasy and QIAshredder kits, reverse transcribed using the SuperScript VILO Reverse Transcription Kit (Invitrogen), and analyzed using Perfecta SYBR Green Fastmix (Quanta BioSciences). All qRT-PCR data are presented as fold change in RNA normalized to *Gapdh* expression. For immunofluorescence staining, cells were fixed with 4% paraformaldehyde, permeabilized with 0.2% Triton X-100, and incubated with primary and secondary antibodies.

### Electrophysiology

A synapsin-RFP lentiviral reporter was used to identify cells in co-culture with primary rat astroglia for patch-clamp analysis at indicated time points. Action potentials and inward and outward currents were recorded in whole-cell configuration. Data were analyzed and prepared for publication using pCLAMP and MATLAB.

### Chromatin Immunoprecipitation qPCR

Chromatin was immunoprecipitated using antibodies against H3K27ac and H3K4me3, and gDNA was purified for qPCR analysis. All sequences for ChIP-qPCR primers can be found in Table S3. qPCR was performed using SYBR green Fastmix (Quanta BioSciences), and the data are presented as fold change gDNA relative to negative control and normalized to a region of the *Gapdh* locus.

### Mouse ENCODE ChIP-Sequencing Datasets

H3K4me3 and H3K27ac ChIP-seq data from C57BL/6 E14.5 whole brain and mouse embryonic fibroblasts (GSE31039) were acquired from the Mouse ENCODE Consortium generated in Bing Ren's laboratory at the Ludwig Institute for Cancer Research.

### Statistical Methods

Statistical analysis was done using GraphPad Prism 7. All data were analyzed with at least three biological replicates and presented as mean  $\pm$  SEM. See figure legends for details on specific statistical tests run and p values calculated for each experiment.

## SUPPLEMENTAL INFORMATION

Supplemental Information includes Supplemental Experimental Procedures, four figures, and three tables and can be found with this article online at <http://dx.doi.org/10.1016/j.stem.2016.07.001>.

## AUTHOR CONTRIBUTIONS

J.B.B., A.F.A., K.W.L., and C.A.G. designed experiments. J.B.B., A.F.A., H.-G.W., A.M.D., and H.A.H. performed the experiments. All authors analyzed the data. J.B.B. and C.A.G. wrote the manuscript with contributions by all authors.

## CONFLICTS OF INTEREST

C.A.G. and J.B.B. are inventors on filed patent applications related to this work.

## ACKNOWLEDGMENTS

The authors thank Ami Kabadi, Pablo Perez-Pinera, and Syandan Chakraborty for providing plasmid constructs; Christopher Grigsby for protocols for PMEFS

transfections and providing the pUNO-Brn2 plasmid; Rui Dai for technical assistance; and Jeff Stogsdill and Cagla Eroglu for supplying astrocytes and providing protocols for co-culture experiments. This work was supported by US NIH grants to C.A.G. and T.E.R. (R01DA036865 and U01HG007900), an NIH Director's New Innovator Award (DP2OD008586) and National Science Foundation (NSF) Faculty Early Career Development (CAREER) Award (CBET-1151035) to C.A.G., and NIH grant P30AR066527. J.B.B. was supported by an NIH Biotechnology Training Grant (T32GM008555).

Received: May 13, 2015

Revised: May 11, 2016

Accepted: June 30, 2016

Published: August 11, 2016

## REFERENCES

- Adler, A.F., Grigsby, C.L., Kulangara, K., Wang, H., Yasuda, R., and Leong, K.W. (2012). Nonviral direct conversion of primary mouse embryonic fibroblasts to neuronal cells. *Mol. Ther. Nucleic Acids* *7*, e32.
- Balboa, D., Weltner, J., Eurola, S., Trokovic, R., Wartiovaara, K., and Otonkoski, T. (2015). Conditionally stabilized dCas9 activator for controlling gene expression in human cell reprogramming and differentiation. *Stem Cell Reports* *5*, 448–459.
- Chakraborty, S., Ji, H., Kabadi, A.M., Gersbach, C.A., Christoforou, N., and Leong, K.W. (2014). A CRISPR/Cas9-based system for reprogramming cell lineage specification. *Stem Cell Reports* *3*, 940–947.
- Chavez, A., Scheiman, J., Vora, S., Pruitt, B.W., Tuttle, M., P R Iyer, E., Lin, S., Kiani, S., Guzman, C.D., Wiegand, D.J., et al. (2015). Highly efficient Cas9-mediated transcriptional programming. *Nat. Methods* *12*, 326–328.
- Cheng, A.W., Wang, H., Yang, H., Shi, L., Katz, Y., Theunissen, T.W., Rangarajan, S., Shivaila, C.S., Dadon, D.B., and Jaenisch, R. (2013). Multiplexed activation of endogenous genes by CRISPR-on, an RNA-guided transcriptional activator system. *Cell Res.* *23*, 1163–1171.
- Cong, L., Ran, F.A., Cox, D., Lin, S., Barretto, R., Habib, N., Hsu, P.D., Wu, X., Jiang, W., Marraffini, L.A., and Zhang, F. (2013). Multiplex genome engineering using CRISPR/Cas systems. *Science* *339*, 819–823.
- Mouse ENCODE Consortium (2012). An encyclopedia of mouse DNA elements (Mouse ENCODE). *Genome Biol.* *13*, 418.
- Davis, R.L., Weintraub, H., and Lassar, A.B. (1987). Expression of a single transfected cDNA converts fibroblasts to myoblasts. *Cell* *51*, 987–1000.
- Gao, X., Yang, J., Tsang, J.C., Ooi, J., Wu, D., and Liu, P. (2013). Reprogramming to pluripotency using designer TALE transcription factors targeting enhancers. *Stem Cell Reports* *1*, 183–197.
- Gao, X., Tsang, J.C., Gaba, F., Wu, D., Lu, L., and Liu, P. (2014). Comparison of TALE designer transcription factors and the CRISPR/dCas9 in regulation of gene expression by targeting enhancers. *Nucleic Acids Res.* *42*, e155.
- Gilbert, L.A., Larson, M.H., Morsut, L., Liu, Z., Brar, G.A., Torres, S.E., Stern-Ginossar, N., Brandman, O., Whitehead, E.H., Doudna, J.A., et al. (2013). CRISPR-mediated modular RNA-guided regulation of transcription in eukaryotes. *Cell* *154*, 442–451.
- Hanna, J., Saha, K., Pando, B., van Zon, J., Lengner, C.J., Creighton, M.P., van Oudenaarden, A., and Jaenisch, R. (2009). Direct cell reprogramming is a stochastic process amenable to acceleration. *Nature* *462*, 595–601.
- Hilton, I.B., D'Ippolito, A.M., Vockley, C.M., Thakore, P.I., Crawford, G.E., Reddy, T.E., and Gersbach, C.A. (2015). Epigenome editing by a CRISPR-Cas9-based acetyltransferase activates genes from promoters and enhancers. *Nat. Biotechnol.* *33*, 510–517.
- Jinek, M., Chylinski, K., Fonfara, I., Hauer, M., Doudna, J.A., and Charpentier, E. (2012). A programmable dual-RNA-guided DNA endonuclease in adaptive bacterial immunity. *Science* *337*, 816–821.
- Kabadi, A.M., Ousterout, D.G., Hilton, I.B., and Gersbach, C.A. (2014). Multiplex CRISPR/Cas9-based genome engineering from a single lentiviral vector. *Nucleic Acids Res.* *42*, e147.
- Kearns, N.A., Pham, H., Tabak, B., Genga, R.M., Silverstein, N.J., Garber, M., and Maehr, R. (2015). Functional annotation of native enhancers with a Cas9-histone demethylase fusion. *Nat. Methods* *12*, 401–413.
- Kim, K., Doi, A., Wen, B., Ng, K., Zhao, R., Cahan, P., Kim, J., Aryee, M.J., Ji, H., Ehrlich, L.I., et al. (2010). Epigenetic memory in induced pluripotent stem cells. *Nature* *467*, 285–290.
- Konermann, S., Brigham, M.D., Trevino, A.E., Hsu, P.D., Heidenreich, M., Cong, L., Platt, R.J., Scott, D.A., Church, G.M., and Zhang, F. (2013). Optical control of mammalian endogenous transcription and epigenetic states. *Nature* *500*, 472–476.
- Ladewig, J., Mertens, J., Kesavan, J., Doerr, J., Poppe, D., Glaue, F., Herms, S., Wernet, P., Kögler, G., Müller, F.J., et al. (2012). Small molecules enable highly efficient neuronal conversion of human fibroblasts. *Nat. Methods* *9*, 575–578.
- Maeder, M.L., Angstman, J.F., Richardson, M.E., Linder, S.J., Cascio, V.M., Tsai, S.Q., Ho, Q.H., Sander, J.D., Reyon, D., Bernstein, B.E., et al. (2013a). Targeted DNA demethylation and activation of endogenous genes using programmable TALE-TET1 fusion proteins. *Nat. Biotechnol.* *31*, 1137–1142.
- Maeder, M.L., Linder, S.J., Cascio, V.M., Fu, Y., Ho, Q.H., and Joung, J.K. (2013b). CRISPR RNA-guided activation of endogenous human genes. *Nat. Methods* *10*, 977–979.
- Mali, P., Aach, J., Stranges, P.B., Esvelt, K.M., Moosburner, M., Kosuri, S., Yang, L., and Church, G.M. (2013a). CAS9 transcriptional activators for target specificity screening and paired nickases for cooperative genome engineering. *Nat. Biotechnol.* *31*, 833–838.
- Mali, P., Yang, L., Esvelt, K.M., Aach, J., Guell, M., DiCarlo, J.E., Norville, J.E., and Church, G.M. (2013b). RNA-guided human genome engineering via Cas9. *Science* *339*, 823–826.
- Mendenhall, E.M., Williamson, K.E., Reyon, D., Zou, J.Y., Ram, O., Joung, J.K., and Bernstein, B.E. (2013). Locus-specific editing of histone modifications at endogenous enhancers. *Nat. Biotechnol.* *31*, 1133–1136.
- Perez-Pinera, P., Kocak, D.D., Vockley, C.M., Adler, A.F., Kabadi, A.M., Polstein, L.R., Thakore, P.I., Glass, K.A., Ousterout, D.G., Leong, K.W., et al. (2013). RNA-guided gene activation by CRISPR-Cas9-based transcription factors. *Nat. Methods* *10*, 973–976.
- Polstein, L.R., Perez-Pinera, P., Kocak, D.D., Vockley, C.M., Bledsoe, P., Song, L., Safi, A., Crawford, G.E., Reddy, T.E., and Gersbach, C.A. (2015). Genome-wide specificity of DNA binding, gene regulation, and chromatin remodeling by TALE- and CRISPR/Cas9-based transcriptional activators. *Genome Res.* *25*, 1158–1169.
- Qi, L.S., Larson, M.H., Gilbert, L.A., Doudna, J.A., Weissman, J.S., Arkin, A.P., and Lim, W.A. (2013). Repurposing CRISPR as an RNA-guided platform for sequence-specific control of gene expression. *Cell* *152*, 1173–1183.
- Takahashi, K., and Yamanaka, S. (2006). Induction of pluripotent stem cells from mouse embryonic and adult fibroblast cultures by defined factors. *Cell* *126*, 663–676.
- Thakore, P.I., Black, J.B., Hilton, I.B., and Gersbach, C.A. (2016). Editing the epigenome: technologies for programmable transcription and epigenetic modulation. *Nat. Methods* *13*, 127–137.
- Treutlein, B., Lee, Q.Y., Camp, J.G., Mall, M., Koh, W., Shariati, S.A., Sim, S., Neff, N.F., Skotheim, J.M., Wernig, M., and Quake, S.R. (2016). Dissecting direct reprogramming from fibroblast to neuron using single-cell RNA-seq. *Nature* *534*, 391–395.
- Vierbuchen, T., and Wernig, M. (2011). Direct lineage conversions: unnatural but useful? *Nat. Biotechnol.* *29*, 892–907.
- Vierbuchen, T., and Wernig, M. (2012). Molecular roadblocks for cellular reprogramming. *Mol. Cell* *47*, 827–838.
- Vierbuchen, T., Ostermeier, A., Pang, Z.P., Kokubu, Y., Südhof, T.C., and Wernig, M. (2010). Direct conversion of fibroblasts to functional neurons by defined factors. *Nature* *463*, 1035–1041.
- Wei, S., Zou, Q., Lai, S., Zhang, Q., Li, L., Yan, Q., Zhou, X., Zhong, H., and Lai, L. (2016). Conversion of embryonic stem cells into extraembryonic lineages by CRISPR-mediated activators. *Sci. Rep.* *6*, 19648.

**Cell Stem Cell, Volume 19**

**Supplemental Information**

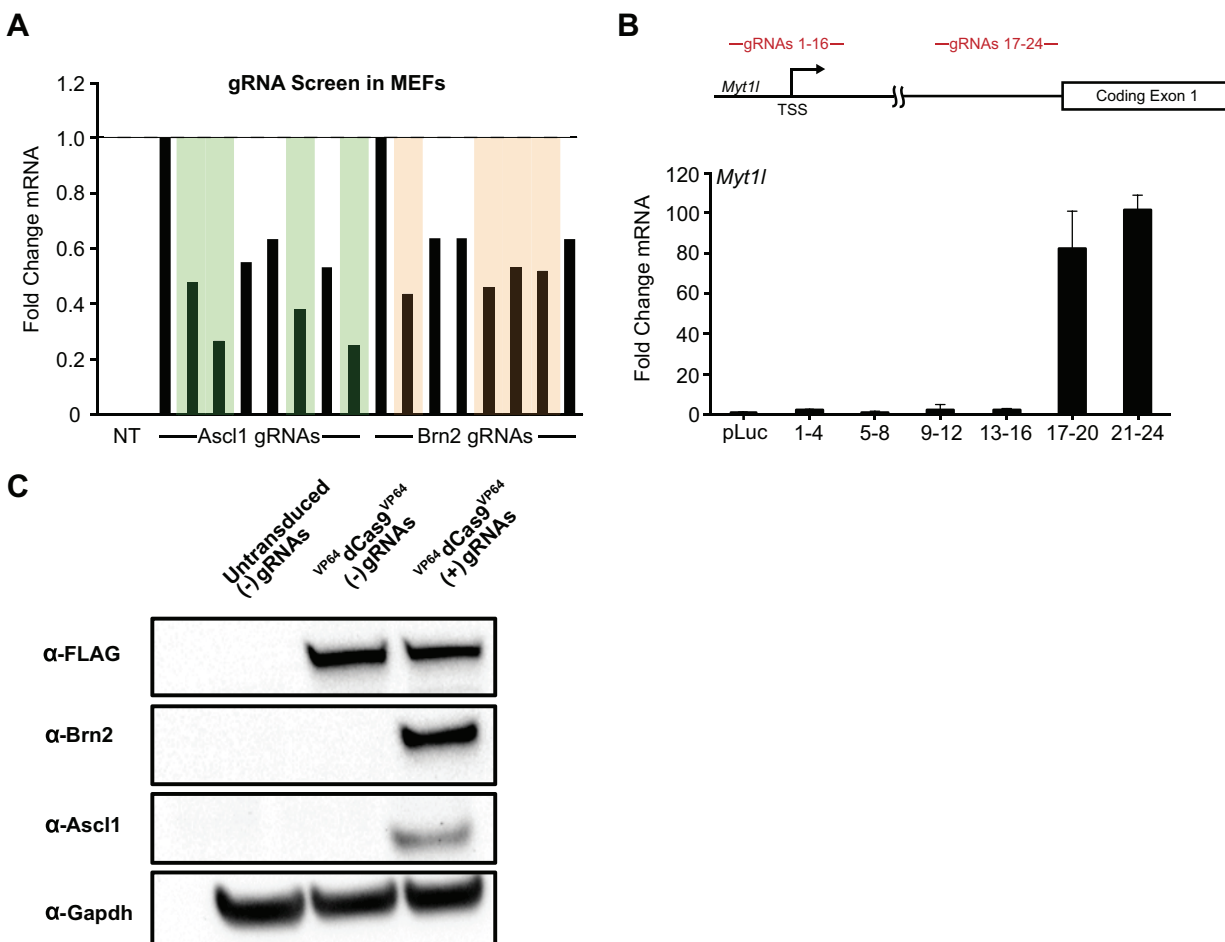
**Targeted Epigenetic Remodeling of Endogenous Loci**

**by CRISPR/Cas9-Based Transcriptional Activators**

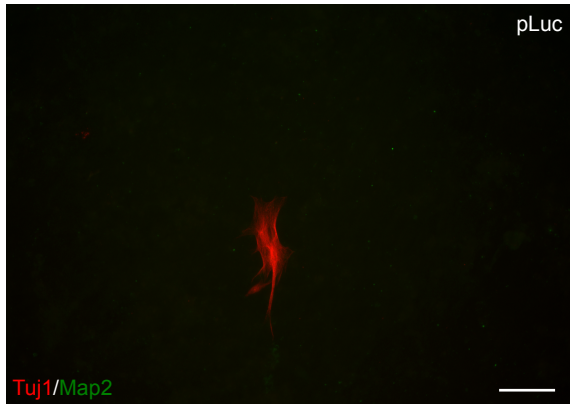
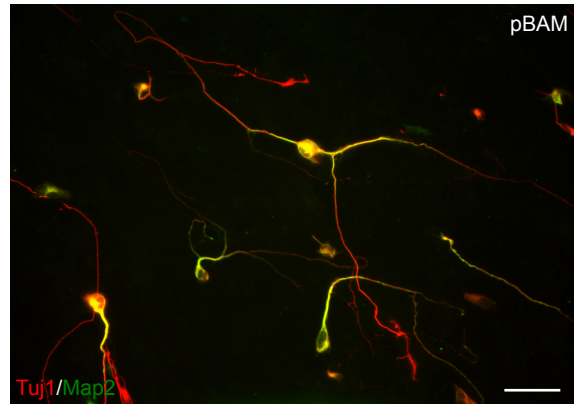
**Directly Converts Fibroblasts to Neuronal Cells**

**Joshua B. Black, Andrew F. Adler, Hong-Gang Wang, Anthony M. D'Ippolito, Hunter A. Hutchinson, Timothy E. Reddy, Geoffrey S. Pitt, Kam W. Leong, and Charles A. Gersbach**

# Supplemental Data



**Figure S1. gRNA optimization and target gene expression in PMEFs (relates to Figure 1).** (A) Selection of gRNAs with highest activity by elimination screening. Each gRNA was eliminated from a pool of eight gRNAs, and the four whose absence resulted in the largest drop in activity were selected for use in this study. (B) Activation of *Myt1l* in PMEFs determined by qRT-PCR with gRNAs targeting an intragenic region adjacent to the first coding exon. Target sites proximal to the TSS did not induce a detectable increase in expression (n = 2 biological replicates). (C) An N-terminal FLAG epitope tag was used to verify expression of <sup>VP64</sup>dCas9<sup>VP64</sup> in transduced PMEFs. Brn2 and Ascl1 protein was only detected in cells transduced with <sup>VP64</sup>dCas9<sup>VP64</sup> and transfected with gRNA expression plasmids.

**A****B**

**Figure S2. Immunofluorescence staining of cells transfected with control plasmids (relates to Figure 2).** (A) PMEFs transfected with firefly luciferase (pLuc) did not generate any Tuj1<sup>+</sup>Map2<sup>+</sup> cells with neuronal morphologies. There were sparse cells with fibroblastic morphologies that stained positive for Tuj1 (scale bar = 50  $\mu$ m). (B) Ectopic expression of the reprogramming factors (pBAM) generated numerous Tuj1<sup>+</sup>Map2<sup>+</sup> cells with elaborate neuronal morphologies (scale bar = 50  $\mu$ m).

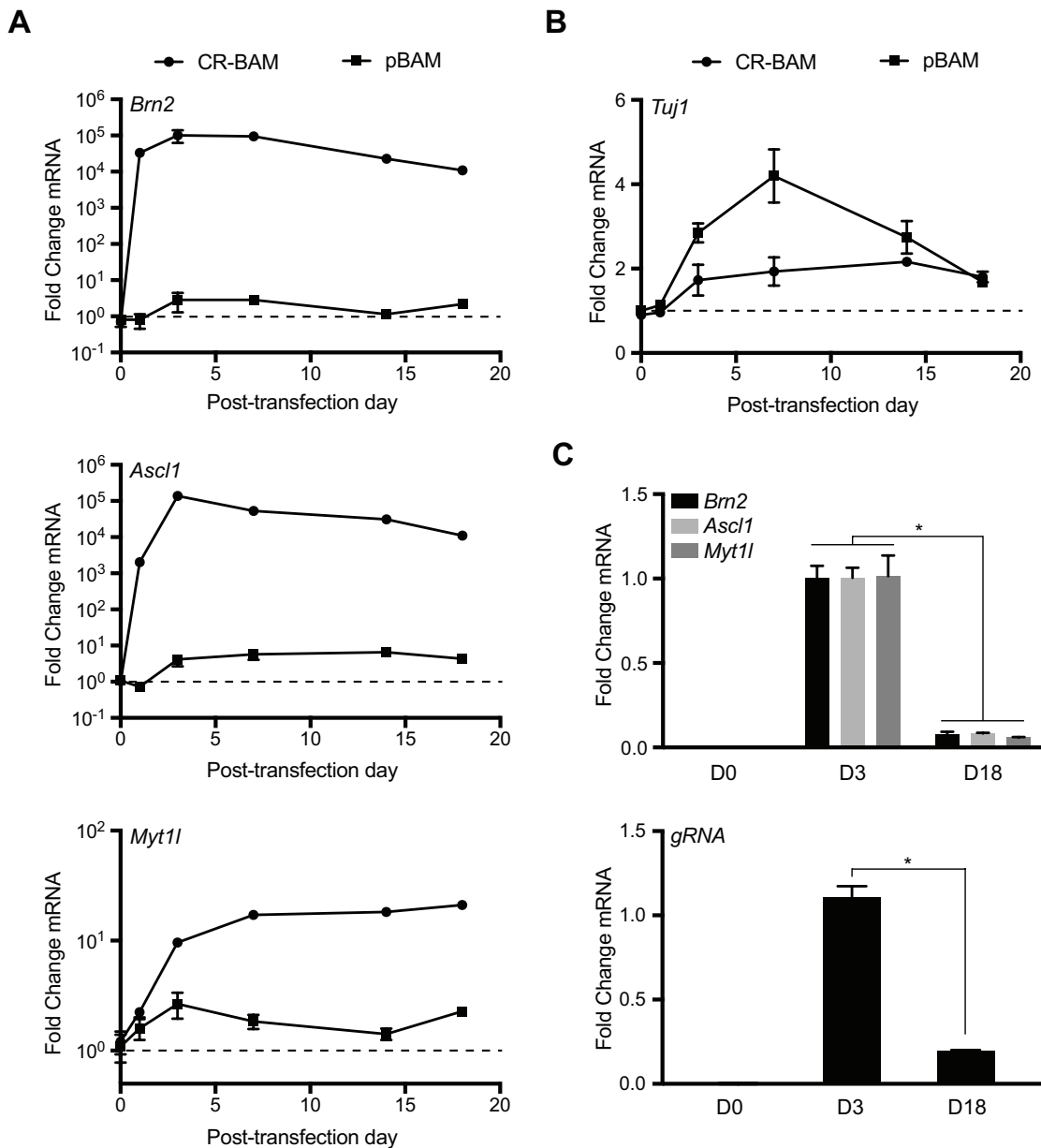


**Figure S3. Targeted Activation Leads to Rapid and Sustained Endogenous Gene Expression (relates to Figure 3).** (A) Activation of the endogenous BAM factors in PMEFs measured by qRT-PCR for 18 days after transfection of gRNAs or ectopic reprogramming factors. Targeted activation of the endogenous genes via  $VP64$ dCas9 $VP64$  and gRNAs is rapid and sustained. Expression of all three endogenous genes is significantly higher with targeted activation than ectopic overexpression throughout the time course of the experiment ( $p < 0.0004$ ). Expression of the factors via ectopic plasmids generated a significant and sustained increase in endogenous *Ascl1* ( $p < 0.0002$ ) and *Myt11* ( $p < 0.0005$ , two-way ANOVA,  $n = 3$  biological replicates). Fold change in mRNA expression is relative to transfection of a plasmid encoding firefly luciferase (pLuc). (B) *Tuj1* mRNA expression is significantly up-regulated throughout the time course of the experiment for both pBAM ( $p < 0.0001$ ) and CR-BAM ( $p < 0.0003$ ) transfection. pBAM transfection induced a higher level of *Tuj1* mRNA than CR-BAM transfection ( $p < 0.02$ , two-way ANOVA,  $n \geq 3$  biological replicates). (C) The ectopic expression vectors for both pBAM (top) and CR-BAM (bottom) transfection are significantly depleted by day 18 post-transfection (pBAM:  $p < 0.002$ , CR-BAM:  $p < 0.0002$ , one-way ANOVA with Holm-Bonferroni post hoc tests,  $n = 3$  biological replicates). The ectopic BAM factors were detected with primers specific to the coding regions of the three genes. The gRNA expression vectors were detected with primers specific to the constant region of the chimeric gRNA sequence (See Table S3 for exact primer sequences).



**Table S1. gRNAs used in this study (relates to all Figures).**

Target Gene	Protospacer Sequence (5' – 3')	Position Relative to TSS	Reference
<i>hASCL1</i> promoter	GCTGGGTGTCCCATTGAAA	-43	Perez-Pinera et al., Nat. Methods, 2013
	CAGCCGCTCGCTGCAGCAG	-103	Perez-Pinera et al., Nat. Methods, 2013
	TGGAGAGTTTGCAAGGAGC	-220	Perez-Pinera et al., Nat. Methods, 2013
	GTTTATTCAGCCGGGAGTC	-284	Perez-Pinera et al., Nat. Methods, 2013
<i>mAscl1</i> promoter	CAGCCGCTCGCTGCAGCAG	-103	Perez-Pinera et al., Nat. Methods, 2013
	TGGAGAGTTTGCAAGGAGC	-202	Perez-Pinera et al., Nat. Methods, 2013
	CCCTCCAGACTTTCCACCT	-392	This study
	CTGCGGAGAGAAGAAAGGG	-523	This study
<i>mBrn2</i> promoter	GAGAGAGCTTGAGAGCGCG	-51	This study
	CCAATCACTGGCTCCGGTC	-185	This study
	GGCGCCCGAGGGAAGAAGA	-222	This study
	GGGTGGGGGTACCAGAGGA	-257	This study
<i>mMyt1l</i> first coding exon	GTCTGGATTCAGTGGACAA	+255188	This study
	TAGAGCTACACAAGATTAA	+255120	This study
	TACCTATGCTGCCCTATGG	+255087	This study
	AGAGCAGGGAGAAGCCTAG	+255023	This study

**Table S2. Plasmids used in this study (relates to all Figures).**

<b>Plasmid Name</b>	<b>Addgene Plasmid #</b>	<b>Reference</b>
pLV-hUbC-dCas9-VP64	53192	Kabadi et al., Nucleic Acids Res., 2014
pLV-hUbC-VP64-dCas9-VP64	59791	Kabadi et al., Nucleic Acids Res., 2014
pLV-4xSPgRNA	N/A	This study
pDM2.G	12259	Trono Lab
psPAX2	12260	Trono Lab
pSPgRNA	47108	Perez-Pinera et al., Nat. Methods, 2013
pUNO1-mBrn2	N/A	This study
pUNO1-mAscl1	N/A	InvivoGen, San Diego, CA
pUNO1-mMyt1b	N/A	InvivoGen, San Diego, CA
VR1255C (pLuc)	N/A	Vical, San Diego, CA
pLV-hSyn-RFP	22909	Nathanson, et al., Neuroscience, 2009
Tet-O-FUW-Ascl1	27150	Vierbuchen et al., Nature, 2010
Tet-O-FUW-Brn2	27151	Vierbuchen et al., Nature, 2010
Tet-O-FUW-Myt1l	27152	Vierbuchen et al., Nature, 2010
FUW-M2rtTA	20342	Hochemeyer et al., Cell Stem Cell, 2008

**Table S3. Quantitative RT-PCR and ChIP-qPCR primers and conditions (relates to all Figures).**

Target	Forward Primer (5' – 3')	Reverse Primer (5' - 3')	Cycling Conditions
endo <i>hASCL1</i>	GGAGCTTCTCGACTTCACCA	AACGCCACTGACAAGAAAGC	95°C 5s 58°C 20s x45
endo <i>mAscl1</i>	GGAACAAGAGCTGCTGGACT	GTTTTTCTGCCTCCCCATTT	95°C 5s 60°C 20s x45
total <i>mAscl1</i>	AGGGATCCTACGACCCTCTTA	ACCAGTTGGTAAAGTCCAGCAG	95°C 5s 60°C 20s x45
endo <i>mBrn2</i>	TTATTTTCCCGGTCCCTTAAA	GTA CTCTCGCCTGCAAAGGT	95°C 5s 60°C 20s x45
total <i>mBrn2</i>	GACACGCCGACCTCAGAC	GATCCGCCTCTGCTTGAAT	95°C 5s 60°C 20s x45
endo <i>mMyt11</i>	CTCGAGAGAGTACCTGCAGAC	AGACCCCCAAATGTGCAGAC	95°C 5s 60°C 20s x45
total <i>mMyt11</i>	CGTGGACTCTGAGGAGAAGC	GTGCATATTTGCCACTGACG	95°C 5s 60°C 20s x45
<i>Tuj1</i>	TCCGAGTACCAGCAGTACCA	GGCTTCCGATTCCTCGTCAT	95°C 5s 64°C 20s x45
<i>gRNA</i>	GCAAGTTAAAATAAGGCTAGTCCG	GACTCGGTGCCACTTTTTTCA	95°C 5s 64°C 20s x45
<i>mGapdh</i>	CCTGCTCCCGTAGACAAAATG	TGAAGGGGTCGTTGATGGC	95°C 5s 60°C 20sx45
<i>hGAPDH</i>	GAAGGTGAAGGTCGGAGTC	GAAGATGGTGATGGGATTTTC	95°C 5s 58°C 20s x45
<i>mBrn2</i> ChIP +2436	AACGCGCATTTAGAGACACG	CAAAGAAGTGCTGATGCCCG	95°C 5s 60°C 20s x45
<i>mBrn2</i> ChIP +1720	ACTCCTCCCCGGCTCAATTA	TGTTTTTATCCCGCCCCAGG	95°C 5s 60°C 20s x45
<i>mBrn2</i> ChIP +1348	GTTACTCAAAGCCAGGGCG	GAATTACAGCGCACAGGTGTC	95°C 5s 60°C 20s x45
<i>mBrn2</i> ChIP +644	AAGGACTGAGAAGACTGGGCG	GCGCCCTTTGATTTACGTGGA	95°C 5s 60°C 20s x45
<i>mBrn2</i> ChIP +130	AACAGAAGGCGTCGGAGC	GGTTAAAGGAGCCGCGCA	95°C 5s 60°C 20s x45
<i>mBrn2</i> ChIP -228	GTTTGCTCTATTTCGAG	GTTGCTGGTGTGGGTGA	95°C 5s 60°C 20s x45
<i>mBrn2</i> ChIP -863	AGACAAGATCGCAGCGCAA	GCTGTAAGCTGTCCGCGA	95°C 5s 60°C 20s x45
<i>mBrn2</i> ChIP -1250	CCACAGTCTTTCCTGGGACC	GTA CTCTCGCCTGCAAAGGT	95°C 5s 60°C 20s x45

Target	Forward Primer (5' – 3')	Reverse Primer (5' – 3')	Cycling Conditions
<i>mAscl1</i> CHIP +2259	TCTGGATCAGGTAGCCCCAG	AAGCAAGTTGCAGTGTGCAG	95°C 5s 60°C 20s x45
<i>mAscl1</i> CHIP +1877	GGGCAGCGGTGATTTATGGA	TCGCTTAGCAACACAAAGCC	95°C 5s 60°C 20s x45
<i>mAscl1</i> CHIP +1482	GACTTTCCACCTAGGCACCC	CGGACTCCCGGCTGAATAAA	95°C 5s 60°C 20s x45
<i>mAscl1</i> CHIP +1230	CGGTTAGGGAGGGCGA	AAAGCAGCCGCAAAG	95°C 5s 60°C 20s x45
<i>mAscl1</i> CHIP +507	CCTCCTTCTGCGCGTTT	CGGCTCCACTCTCCAT	95°C 5s 60°C 20s x45
<i>mAscl1</i> CHIP +145	TCGTCCTCTCCGGAAGTAT	GTGGCAAACCCAGGTTGAC	95°C 5s 60°C 20s x45
<i>mAscl1</i> CHIP -314	TCCCCAACTACTCCAA	CCACATGAAGCGTACC	95°C 5s 60°C 20s x45
<i>mMyt1l</i> CHIP -1821	GCTCCTTGTGGAGTGGAGTC	TCTCTCTGAGCTGTGGCTCT	95°C 5s 60°C 20s x45
<i>mMyt1l</i> CHIP -965	AGAATCGAGCAATCCGTCCC	TGGCTTACTGCCTTTCGGTT	95°C 5s 60°C 20s x45
<i>mMyt1l</i> CHIP -665	ATTTTGCAGGATGTCCCCCT	GGTTTCATGAAGACCGGCT	95°C 5s 60°C 20s x45
<i>mMyt1l</i> CHIP +210	CCCTGCAGTCTTCTTGGAGG	GGCAGGGAAGGTTGCTTTTG	95°C 5s 60°C 20s x45
<i>mMyt1l</i> CHIP +255049	AGAGGAGAGCTGGATCCCTG	GCCTCCATAGGGCAGCATAG	95°C 5s 60°C 20s x45
<i>mMyt1l</i> CHIP +261083	CAGCCGGTGGGTGAATAATTG	CAGAATCCAAATGAGGCGTGC	95°C 5s 60°C 20s x45
<i>mGapdh</i> CHIP +611	GTATTAGGAACAACCCACGC	TATGCACCTCACAACGCCAT	95°C 5s 60°C 20s x45

# Supplemental Experimental Procedures

**Lentiviral Production.** HEK293T cells were acquired from the American Tissue Collection Center (ATCC) and purchased through the Duke University Cancer Center Facilities and were cultured in Dulbecco's Modified Eagle's Medium (Invitrogen) supplemented with 10% FBS (Sigma) and 1% penicillin/streptomycin (Invitrogen) at 37°C with 5% CO<sub>2</sub>. Approximately 3.5 million cells were plated per 10 cm TCPS dish. Twenty-four hours later, the cells were transfected using the calcium phosphate precipitation method with pMD2.G (Addgene #12259) and psPAX2 (Addgene #12260) second generation envelope and packaging plasmids. The medium was exchanged 12 hours post-transfection, and the viral supernatant was harvested 24 and 48 hours after this medium change. The viral supernatant was pooled and centrifuged at 600 g for 10 minutes, passed through a 0.45 µm filter, and concentrated using Lenti-X Concentrator (Clontech) in accordance with the manufacturer's protocol.

**Cell Culture, Transductions and Transfections.** For lentiviral transduction of <sup>VP64</sup>dCas9<sup>VP64</sup> (Addgene #59791), 40,000 PMEF-HL (Millipore) cells were plated into viral supernatant with 4 µg/ml polybrene and incubated for 20-24 hours before medium exchange. The cells were cultured for an additional three days in PMEF medium: Dulbecco's Modified Eagle's Medium (Invitrogen), 10% FBS (Sigma), 25 µg/ml gentamicin (Invitrogen), and 1x sodium pyruvate, GlutaMAX, nonessential amino acids, and β-mercaptoethanol (Invitrogen). The cells were then re-plated for transfection at 100,000 cells per well of a 24-well TCPS plate. Twenty-four hours after plating, the cells were transfected with either pmax-GFP to monitor efficiency, VR1255C (pLuc) to serve as a negative control, pUNO-BAM to serve as a positive control, or CR-BAM gRNA plasmid cocktails. Transfections were carried out using Lipofectamine 3000 (Invitrogen) in accordance with the manufacturer's protocol. Briefly, Lipofectamine 3000 and DNA (0.5 µg DNA per well of 24-well TCPS plate) were mixed at a 3:1 volume-to-mass ratio in serum-free Opti-MEM (Invitrogen). Transfections were carried out in complete PMEF medium with antibiotic for 12-15 hours before exchanged for fresh PMEF medium. Twenty-four hours later, PMEF medium was replaced with N3 neural induction medium: DMEM/F-12 Nutrient Mix (Invitrogen), B-27 serum-free supplement (Invitrogen), N-2 serum-free supplement (Invitrogen), 10 µM SB-431542 (Sigma), 0.5 µM LDN-193189 (Sigma), 2 µM CHIR99021 (Stemgent), and 25 µg/ml gentamicin (Invitrogen). The medium was half-exchanged every 48 hours for the first 10 days, and then every 24 hours for the remainder of the time in culture.

For experiments requiring stable integration of all expression vectors, PMEF-CD-1 (Stemcell) cells were thawed once and transduced following the protocol described previously. PMEFs were either transduced with vectors directly encoding the BAM factors under the control of doxycycline-inducible promoters (Addgene #27150, #27151 and #27152) along with the reverse tetracycline-controlled transactivator (Addgene 20342) or with <sup>VP64</sup>dCas9<sup>VP64</sup> (Addgene #59791) and multiplex gRNA vectors (this study) and cultured in neurogenic medium. For electrophysiological analysis, cells were transduced with Syn-RFP (Addgene #22909) and were dissociated after 7-15 days in culture using Accutase (Stemcell) and replated onto a previously established monolayer of primary rat astrocytes on poly-D-lysine/laminin-coated glass coverslips (BD) and cultured for an additional 7 – 12 days. The medium was half-exchanged every 3 days.

**Glia cell isolation.** The cortices from postnatal day one Sprague-Dawley rat pup brains were dissected and sectioned into 1 mm<sup>3</sup> pieces. The tissue was incubated with a papain solution (1 vial papain (Worthington) in 20 ml D-PBS (Gibco) with 200 µl 0.4% DNase) for 45 minutes at 37°C. The solution was mixed by swirling every 15 minutes. The dissociated tissue was collected with repeated incubations with a low ovomucoid solution (2 ml 10X Low Ovo stock (Worthington) in 18 ml D-PBS with 200 µl 0.4% DNase) and a high ovomucoid solution (2 ml 6X High Ovo stock (Worthington) in 10 ml D-PBS). The cell mixture was centrifuged twice at 1100 rpm for 11 minutes, filtered through a 30 µm Nitex membrane, and centrifuged a final time and resuspended in Astrocyte Growth Media (500 ml DMEM (Gibco), 50 ml heat inactivated FCS (Gibco), 5 ml pen-strep (Gibco), 2 mM glutamine (Gibco), 1 mM sodium pyruvate (Gibco), 5 µg/ml NAC (Sigma), 5 µg/ml insulin (Sigma), and 10 µM hydrocortisone (Sigma)). Contaminating cells were removed by vigorous shaking and the addition of 10 µM Ara-C. The astrocytes were passaged two times before culturing with PMEF-derived iNs.

**Quantitative Reverse Transcription PCR.** Cells were lysed directly from a 24-well TCPS plate, and total RNA was isolated using RNeasy Plus and QIAshredder kits (Qiagen). Reverse transcription was carried out on 0.5 µg total RNA per sample in a 10 µl reaction using the SuperScript VILO Reverse Transcription Kit (Invitrogen). 1.0 µl of cDNA was used per PCR reaction with Perfecta SYBR Green Fastmix (Quanta BioSciences) using the CFX96 Real-Time PCR Detection System (Bio-Rad). The amplification efficiencies over the appropriate dynamic range of all primers were optimized using dilutions of purified amplicon in Herring Sperm DNA (Invitrogen). All amplicon products were verified by gel electrophoresis and melting curve analysis. All qRT-PCR results are presented as fold change in mRNA normalized to *Gapdh* expression.

**Western Blot.** Cells were lysed with RIPA buffer (Sigma) containing a protease inhibitor cocktail (Sigma). Protein concentration was assessed using a bicinchoninic acid (BCA) protein standard curve (Thermo Scientific) on the BioTek Synergy 2 Multi-Mode Microplate Reader. 25 µg of protein per sample was loaded into a NuPage 4-12% Bis-Tris Gel polyacrylamide gel (Invitrogen) and transferred to a nitrocellulose membrane. Following transfer, the membrane was washed briefly with TBST (50 mM Tris, 150 mM NaCl and 0.1% Tween-20) and blocked for 1 hour at room temperature in TBST with 5% nonfat milk. The membrane was washed three times for 15 minutes and then incubated with primary antibody in blocking solution overnight at 4° C. The following primary antibodies were used: rabbit anti-FLAG (1:1000 dilution, Sigma, F7425); rabbit anti-Brn2 (1:1000 dilution, abcam, ab94977); goat anti-Ascl1 (1:200 dilution, Santa Cruz, sc-48449); rabbit anti-GAPDH (1:5000 dilution, Cell Signaling, clone 14C10). The membrane was washed three times for 15 minutes and then incubated with secondary antibody in blocking solution for 1 hour at room temperature. The following secondary antibodies were used: anti-rabbit HRP-conjugated (1:5000 dilution, Sigma, A6154); anti-goat HRP-conjugated (1:5000 dilution, Santa Cruz, sc-2354). The membrane was washed with TBST for 1 hour at room temperature and then imaged using the ImmunStar WesternC Chemiluminescence Kit (Bio-Rad) and ChemiDoc XRS+ System (Bio-Rad).

**Immunofluorescence Staining and Image Analysis.** Cells were washed briefly with PBS and then fixed with 4% paraformaldehyde (Sigma) for 20 minutes at room temperature. Cells were washed twice with PBS and then incubated with blocking buffer (10% FBS (Sigma), 3% wt/vol BSA, and 0.2% Triton X-100) for 30 minutes at room temperature. The following primary antibodies were used with incubations overnight at 4 °C: rabbit anti-Brn2 (1:500 dilution, Abcam, ab94977); goat anti-Ascl1 (1:100 dilution, Santa Cruz, sc-48449); rabbit anti-Tuj1 (1:500 dilution, Covance); mouse anti-Map2 (1:500 dilution, BD Biosciences). Cells were washed three times with PBS and then incubated with secondary antibody in blocking solution for 1 hour at room temperature. The following secondary antibodies were used: Alexa Fluor 488 goat anti-rabbit (1:500 dilution, Invitrogen); Alexa Fluor 594 goat anti-mouse (1:500 dilution, Invitrogen); Alexa Fluor 594 donkey anti-goat (1:500 dilution, Invitrogen). Cells were washed three times with PBS and imaged with a Leica DMI 3000 B fluorescence microscope.

Quantification of single-cell Brn2 and Ascl1 protein levels in transfected cells was assessed using a MATLAB script. Briefly, DAPI images were used to identify nuclei, and the mean fluorescence within the nucleus was recorded for the channels corresponding to Brn2 and Ascl1. Distributions of mean intensities were constructed by collecting all cells with intensities greater than two standard deviations above the mean intensity of cells transfected with firefly luciferase. Tuj1<sup>+</sup>Map2<sup>+</sup> and Tuj1<sup>+</sup>Syn-RFP<sup>+</sup> cells were counted manually from images at 10x magnification. Counting was performed on 10 randomly selected windows from 3 biological replicates for each treatment condition.

**Electrophysiology.** RFP expression from the Syn-RFP lentiviral reporter was used to identify the most mature iNs for patch clamping using a Nikon2000-U fluorescence microscope. Evoked action potentials and inward and outward currents were recorded in whole-cell configuration using an Axopatch 200B amplifier (Molecular Devices). The intracellular solution contained 120 mM potassium gluconate, 10 mM KCl, 5 mM MgCl<sub>2</sub>, 0.6 mM EGTA, 5 mM HEPES, 0.006 mM CaCl<sub>2</sub>, 10 mM phosphocreatine disodium, 2 mM Mg-ATP, 0.2 mM GTP, and 50 units/ml creatine phosphokinase, pH 7.3 adjusted with KOH. The extracellular solution contained 119 mM NaCl, 5 mM KCl, 20 mM HEPES, 2 mM CaCl<sub>2</sub>, 2 mM MgCl<sub>2</sub>, 30 mM glucose, pH 7.3 adjusted with NaOH. Data were analyzed and prepared for publication using pCLAMP and MATLAB.

**Chromatin Immunoprecipitation qPCR.** For transfection experiments, cells were transfected in 15 cm TCPS dishes and cultured in neurogenic medium for three days before fixation. For transduction experiments, cells were transduced in 15 cm TCPS dishes and fixed after 3 and 6 days post-transduction. Cells were fixed in 1% formaldehyde for 10 minutes at room temperature. The reaction was quenched with 0.125 M glycine, and the cells were lysed using Farnham lysis buffer with a protease inhibitor cocktail (Roche). Nuclei were collected by centrifugation at 2,000 rpm for 5 minutes at 4°C and lysed in RIPA buffer with a protease inhibitor cocktail (Roche). The chromatin was sonicated using a Bioruptor Sonicator (Diagenode, model XL) and immunoprecipitated using the following antibodies: anti-H3K27ac (abcam, ab4729) and anti-H3K4me3 (abcam, ab8580). The formaldehyde crosslinks were reversed by heating overnight at 65°C, and genomic DNA fragments were purified using a spin column. qPCR was performed using SYBR Green Fastmix (Quanta BioSciences) with the CFX96 Real-Time PCR Detection System (Bio-Rad). 500 pg of genomic DNA was used in each qPCR reaction. The data are presented as fold change gDNA relative to negative control and normalized to a region of the Gapdh locus. Primers were designed to target regions with H3K27ac and/or H3K4me3 enrichment in mouse embryonic day 14.5 brain tissue (Figures 3 and S4).

## Supplemental References

Nathanson, J.L., Yanagawa, Y., Obata, K., and Callaway, E.M. (2009). Preferential labeling of inhibitory and excitatory cortical neurons by endogenous tropism of adeno-associated virus and lentivirus vectors. *Neuroscience* *161*, 441-450.

Hockemeyer, D., Soldner, F., Cook, E.G., Gao, Q., Mitalipova, M., Jaenisch, R. (2008). A drug-inducible system for direct reprogramming of human somatic cells to pluripotency. *Cell Stem Cell* *3*(3):346-353.